Chapter 2
Plant Electrostimulation and Data Acquisition

Emil Jovanov and Alexander G. Volkov

Abstract Plant electrostimulation is a very efficient method for evaluation of biologically closed electrical circuits in plants. The information gained from plant electrostimulation can be used to elucidate and observe the intracellular and intercellular communication in the form of electrical signals within plants. Monitoring the electrical signaling in higher plants represents a promising method to investigate fast electrical communication during environmental changes. Here we discuss DC methods of plant electrostimulation and describe a new Charge Stimulation Method in plant electrophysiology. It is often convenient to represent the real electrical and electrochemical properties of biointerfaces with idealized equivalent electrical circuit models consisting of discrete electrical components. Biologically closed electrical circuits in plants can be investigated using the Charge Stimulation Method.

2.1 Introduction

The electrical phenomena in plants have attracted researchers since the eighteenth century (Bertholon 1783; Bose 1907, 1913, 1918, 1926, 1928; Burdon-Sanderson 1873; Davies 2006; Keller 1930; Ksenzhek and Volkov 1998; Lemström 1904;

E. Jovanov (✉)
Electrical and Computer Engineering Department,
University of Alabama in Huntsville, Huntsville, AL 35899, USA
e-mail: emil.jovanov@uah.edu

A. G. Volkov
Department of Chemistry, Oakwood University,
7000 Adventist Blvd, Huntsville, AL 35896, USA
e-mail: agvolkov@yahoo.com

A. G. Volkov (ed.), *Plant Electrophysiology*,
DOI: 10.1007/978-3-642-29119-7_2, © Springer-Verlag Berlin Heidelberg 2012

Sinukhin and Britikov 1967; Volkov 2006a, b). Biologically closed electrical circuits (Nordestrom 1983) operate over large distances in biological tissues. The activation of such electrical circuits can lead to various physiological and biochemical responses. The cells of many biological organs generate electric potentials that can result in the flow of electric currents (Volkov et al. 1998). Electrical impulses may arise as a result of stimulation. Once initiated, these impulses can propagate to adjacent excitable cells. The change in transmembrane potential can create a wave of depolarization which affects the adjoining, resting membranes. Thus, while the plasma membrane is stimulated at any point, the action potential can propagate over the entire length of the cell membrane and along the conductive bundles of tissue with constant amplitude, duration, and speed (Volkov 2006b). Characteristic length of action potentials is defined as the propagation speed multiplied by the duration of the action potential. To detect the real action potentials, the distance between electrodes should exceed the characteristic length of an action potential. Graded, electrotonic, and variation potentials propagate with decreasing amplitude. Electrical signals can propagate along the plasma membrane on short distances in plasmodesmata, and on long distances in conductive bundles. Action potentials in higher plants hold promise as the information carriers in intracellular and intercellular communication during environmental changes (Volkov 2000, 2006b).

Measurement of plant electrical activity and evoked potentials raise a number of challenging issues, including type and position of electrodes, reference potentials, methodology of measurement, and synchronization with external events. Omissions and mistakes in methodology may lead to incorrect conclusions about the nature of underlying processes. One of the typical mistakes is creating direct analogies between standard electrical circuits and electrical circuits in plants. Electrical circuits have clearly defined reference potential ("common ground") and all potentials are measured relative to the ground potential. Most potentials in computer systems are digital and exhibit high immunity to noise. In contrast, plants exhibit a hierarchical structure with no common ground potential, many signals are nonlinear, and have poor signal to noise ratio.

Scientific hypotheses could be tested using electrical stimulation of plants and monitoring of biological effects caused by the stimulation.

In this chapter we present methods for monitoring and stimulation of plant's electrical activity. In addition to fundamental theoretical concepts we present our experience in the configuration and development of the custom data acquisition and plant DC stimulation systems, and results from plant experiments.

2.2 Data Acquisition

Although many processes in plants are slow enough for direct observation, a number of processes are too quick and require additional instrumentation for scientific study. Typical example is mechanical closing of carnivorous plants, such as the Venus

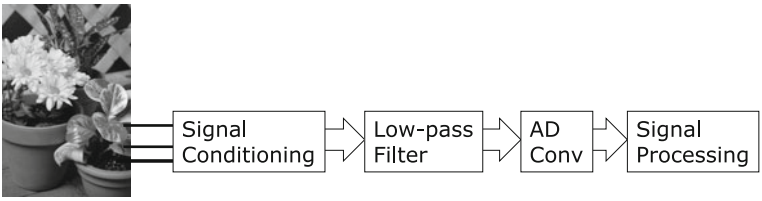

Fig. 2.1 Block diagram of the data acquisition system

flytrap, that can close lobes and capture small insects in a fraction of the second (Markin et al. 2008; Volkov et al. 2007, 2008a, b). In addition to fast cameras, it is necessary to monitor electrical activity and plant signaling during closing.

Data acquisition is the process of converting analog physical signals into digital numeric values that can be stored, processed, and visualized by a computer. Data acquisition systems are often represented by the acronyms DAS or DAQ. Recent development of embedded computer systems and standard data acquisition boards lead to the development of virtual instrumentation that allows use of common hardware with custom software to represent virtual instruments for a variety of applications.

Typical components of data acquisition systems include:

- *Sensors* that convert physical parameters to electrical signals that can be processed by the data acquisition system,
- *Signal conditioning circuits* to convert sensor signals into a form that can be converted to digital values,
- *Analog-to-digital converters*, which convert conditioned sensor signals to digital values,
- *Microprocessor-based controller* that performs the following functions:
  - user interface and control,
  - file access and storage,
  - networking for distributed systems,
  - signal processing and analysis, and
  - result presentation and visualization

For example, a digital thermometer might use thermistor as *sensor* to convert temperature to variable resistance; *signal conditioning circuit* (such as voltage divider or amplifier) to convert variable resistance to variable voltage, amplify and filter signal; *analog-to-digital converter* can be used to convert the voltage to digital values that are read and processed by the microcontroller, and displayed to the user.

Analog-to-digital conversion assumes analog voltages relative to the reference voltage.

Data acquisition applications are typically controlled by application-specific programs that provide custom user-interfaces, processing, and presentation of results (Fig. 2.1).

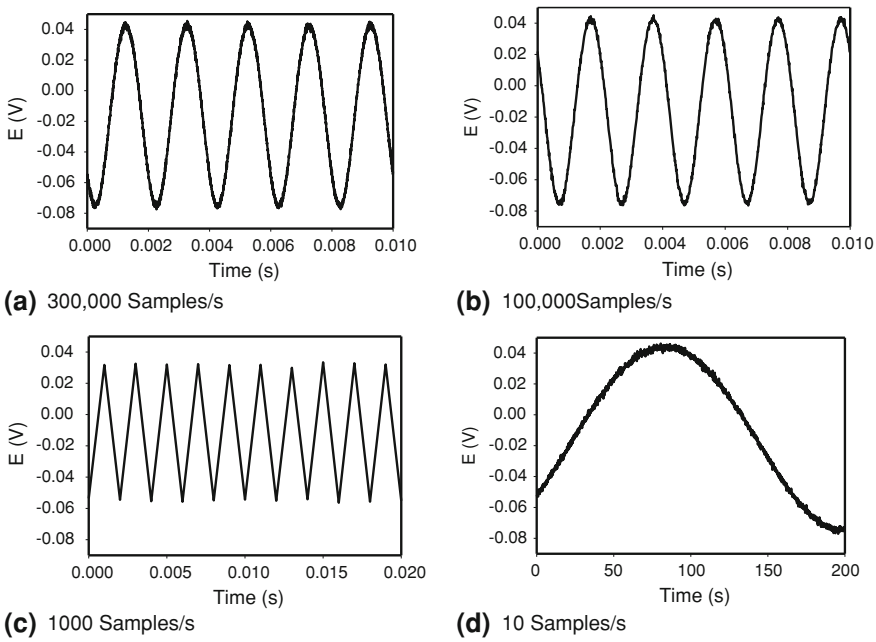

Fig. 2.2 Reconstructed 500 Hz sinusoidal signal from the digitized signal sampled at **a** 300,000 samples/second, **b** 100,000 samples/second, **c** the Nyquist rate of 1,000 samples/second; **d** aliased 500 Hz signal due to under sampling at 10 samples/second

2.2.1 Sampling

Sampling represents the process of converting continuous analog signals with unlimited time and amplitude resolution to discrete samples equivalent to the instantaneous value of the continuous signal at the desired time points. Typical sampling of the analog signal is represented in Fig. 2.2. Sampling involves time and amplitude discretization, as described in the following sections.

2.2.1.1 Time Discretization

Continuous analog signal is converted to a sequence of discrete samples in discrete time points that could be uniform or variable. Uniform sampling is commonly used, where the sampling interval T_s determines sampling frequency or sampling rate F_s:

$$F_s = \frac{1}{T_s} \tag{2.1}$$

Sampling frequency determines the number of samples obtained in one second, represented in samples per second or expressed in Hertz (Hz). For example,

sampling frequency $F_s = 100$ Hz means that we will collect 100 samples of the signal per second.

Fundamental limitation of sampling is represented by Nyquist–Shannon sampling theorem (Shannon 1949) which shows that a sampled analog signal can be perfectly reconstructed from an infinite sequence of samples if the sampling rate exceeds $2 \cdot F_{max}$ samples per second, where F_{max} represents the highest frequency of the original signal, also known as Nyquist frequency:

$$F_s \geq 2 F_{max} \tag{2.2}$$

Therefore, data acquisition systems must satisfy two conditions:

- The signal conditioning circuit must limit maximum frequency of the signal to $F_{s\ max}$ [Hz]; typically, this is implemented as a low pass or band pass filter with maximum cutoff frequency of $F_{s\ max}$ [Hz]. Please note that even without periodic high-frequency components, fast changing signals have wide spectrum (theoretically infinite spectrum) that must be limited for correct data acquisition.
- The data acquisition card must sample signals with sampling rate of at least $2 \cdot F_{max}$ [Hz]. However, lower cutoff frequency of the low pass filter may distort the signal in the presence of fast changing signals (see previous condition); hence, cutoff frequency of the low pass filter is usually selected close to $F_s/2$.

Consequently:

> Sampling frequency F_s is selected to preserve most of the frequency content and shape of the signal, and data acquisition systems must use low pass filter with cutoff frequency not higher than $F_s/2$.

Figure 2.3 represents an example of inadequate sampling frequency and wrong conclusions that might be drawn from the measurement. A sequence of fast regular pulses sampled at low frequency might generate the impression that the underlying phenomenon is a single, slow changing pulse, as represented in the lower plot of Fig. 2.3.

General purpose voltmeters typically represent slow data acquisition systems with sampling rate in the order of few samples per second. Therefore, some high speed changes might generate false impression of the underlying phenomena, as represented in Fig. 2.3.

2.2.1.2 Quantization and Coding

Analog samples are converted to digital values using Analog-to-Digital or AD Converters. AD converter represents a quantizer with a number of discrete levels against which the sampled amplitude is compared to generate a binary code representing amplitude of the current sample. The number of levels is defined by the resolution or number of bits (nb) of the AD converter. The value of the

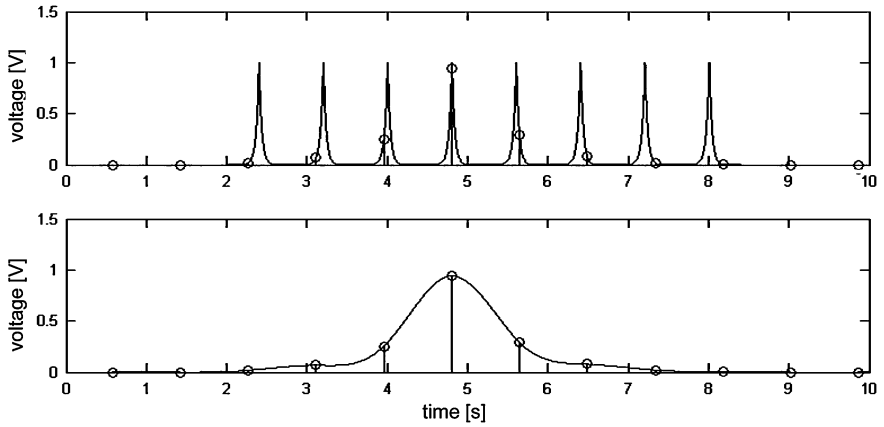

Fig. 2.3 Illustration of data acquisition with inadequate sampling frequency; *upper plot* synthetic signal as a sequence of pulses; *lower plot* reconstructed signal sampled with low sampling frequency

quantization step Δ depends on the range and resolution of the AD converter and can be represented as:

$$\Delta = \frac{V^+ - V^-}{2^{\text{nb}}} \tag{2.3}$$

where V^+ and V^- represent positive and negative reference voltages, and $V_{\text{range}} = V^+ - V^-$. For example, a 12-bit AD converter with $V^+ = 5$ V and $V^- = 0$ V has quantization step of:

$$\Delta = \frac{5\,\text{V} - 0\,\text{V}}{2^{12}} = \frac{5\,\text{V}}{4096} = 1.22\,\text{mV} \tag{2.4}$$

Error generated by the quantization can be represented as a noise generated by conversion. For the truncation quantizer the maximum error can be represented as:

$$0 \leq \varepsilon \leq \Delta = \frac{V_{\text{range}}}{2^{\text{nb}}} \tag{2.5}$$

Therefore, signal to noise ratio and maximum noise can be controlled by the resolution of the AD converter. Quantization and coding are represented in Fig. 2.4.

If a single AD converter is used for multiple signals (multichannel configuration), individual channels might use separate references (*differential input*) or a single reference for all channels (*single ended*). Noise immunity is much better with differential input, while single ended recording allows two times more channels in the same data acquisition setup.

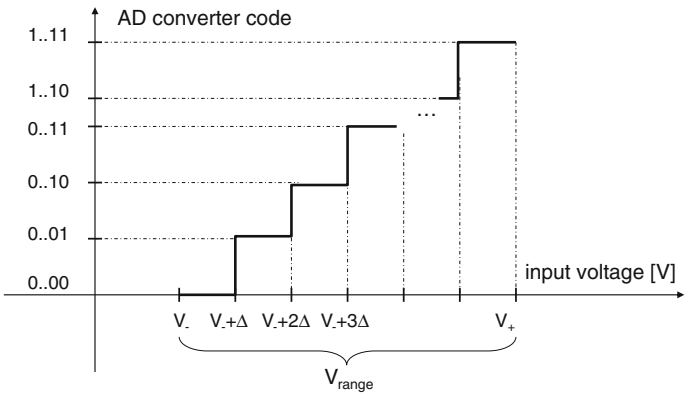

Fig. 2.4 Quantization and coding

2.2.2 Signal Conditioning

Monitoring of electrical activity of plants creates several unique challenges:

- plant's electrical activity generates very small voltages, typically in the order of mV or tens of mV
- sources of plant's electrical activity are very weak and must be amplified to improve noise immunity of the signals
  - amplifiers also need a reference point (referenced as "GROUND" in typical electrical systems); however, choice of the reference point may significantly influence signal generation and signal quality. The most convenient reference point is soil around the plant; however, in many applications this configuration is inadequate due to large resistance between sources of plant activity and root/soil around the plant.
  - separate source ground and measurement system grounds create difference in ground potentials and ground loops, visible mostly as power line interference (50 Hz in Europe or 60 Hz in America).
- long wires typically require differential acquisition or optical isolation of sources of plant activity.

2.2.3 Impedance Matching

Sources of plant electrical activity can be represented as ideal voltage source with series resistance, as represented in Fig. 2.5. Measured voltage (V_m) will depend on the resistance of electrodes (R_e), as well as input resistance of the measurement device (R_{in}) and can be represented as:

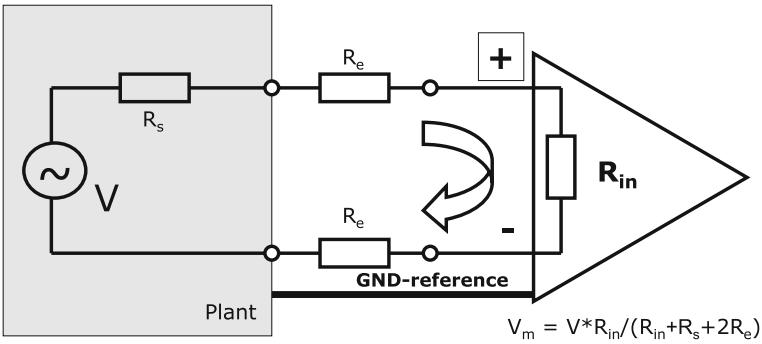

Fig. 2.5 Measured potential as a function of the internal resistance of the measurement equipment; R_e—electrode impedance, R_s—source impedance, R_{in}—input impedance of the measurement system

$$V_m = V_s \frac{R_{in}}{R_{in} + R_s + 2R_e} = V_s \frac{1}{1 + \frac{R_s}{R_{in}} + \frac{2R_e}{R_{in}}} \tag{2.6}$$

For very large values of the input resistance $(R_{in} \to \infty)$, $V_m \approx V_s$.

Typical values for R_e are in the order of a few kΩ for Ag/AgCl electrodes and tens of MΩ for ion selective electrodes with membranes, while R_s is often in the order of hundreds or thousands of kΩ. Therefore, input resistance of the data acquisition system must be at least in the order of GΩ to accurately represent the signal. That is the reason why low input resistance oscilloscopes cannot be used without signal conditioning and amplification of the signal.

2.3 DC Methods of Electrostimulation

There are a few "methods" of plant electrostimulation such as using DC source of voltage or electrical current (Houwink 1935, 1938; Jonas 1970; Mizuguchi et al. 1994; Volkov et al. 2007), function generator (Volkov et al. 2012), charge stimulation method (Volkov et al. 2008a, b, c, 2009a, b, 2010a, b, c, d, 2011a, b, c, d) or AC method of electrical impedance (Inaba et al. 1995; Laarabi et al. 2005; Wang et al. 1994; Zhang and Willison 1991).

2.3.1 Function Generator

Function generators are routinely used for stimulation of the general purpose electrical circuits. The function generator gives many options for the electrostimulation: shapes, duration, frequency of stimulation, and offset voltage U_{offset}, but it cannot regulate the electrical charge or electrical current during the plant electrostimulation.

Function generator actively drives all states of the generated signal. For example, for a square wave signal, function generator will generate inactive states as voltage equal to 0 V and active state at a certain voltage (e.g., 1 V output). This means that the function generator connected to the plant will actively force 0 V voltage even during inactive state that will in most cases interfere with the resting state of the plant (approximately 20–60 mV generated by the plant). Similarly, when a function generator is used to apply pulses with a given potential, it generates a potential of zero volts when the pulse is not being applied. For example, when the generator applies a 100 mV pulse lasting for 1 s, the function generator will generate a 0 mV output before and after the pulse. This means that the native plant potential will be forced to zero during periods of no stimulation, which interferes with the normal plant signaling mechanism and electrical recovery of the plant.

Therefore, stimulation using function generator interferes with the electrical recovery of the plant. That is the reason why we used charge stimulation method.

2.3.2 Charge Stimulation Method

Charged capacitor applies electrical potential between two electrodes decreasing gradually to zero during the discharge of a capacitor. A function generator maintains a given high or low potential in the electrodes. For this reason, the electrical response during the potential increase or decrease from a function generator has corresponding positive or negative amplitude. Therefore, in order to estimate the plant's response after stimulation, we have to effectively "disconnect" the function generator from the plant and monitor the plant's electrical response. This feature is not available with standard function generators. We propose the use of the charge stimulation method that allows delivery of an electrical charge and disconnection from the plant. The charge is delivered from a capacitor that is charged at a given potential. When a capacitor with capacitance C is connected to the source with potential voltage U, the total capacitor charge is $Q = CU$, which allows precise regulation of the amount of charge during stimulation by using different capacitors and applying various voltages. A mechanical or electronic switch can instantaneously connect the charged capacitor to the plant and induce a response for a given stimulation period and disconnect the capacitor to monitor the plant's response (Volkov et al. 2010b, 2011a).

We applied a novel electrostimulation method, as presented in Fig. 2.6, to allow separate control of both amplitude and timing of the stimulation pulse and to provide a high-impedance optical isolation when the plant is not stimulated. We used a custom board with microcontroller *Texas Instruments* MSP430F149 to generate logic pulse of the precisely controlled duration on user's request. The pulse triggers a signal conditioning circuit with preset reference voltage through the optocoupler. This approach effectively disconnects the plant from the stimulation system when the pulse is not present. The amplifier allows active driving of

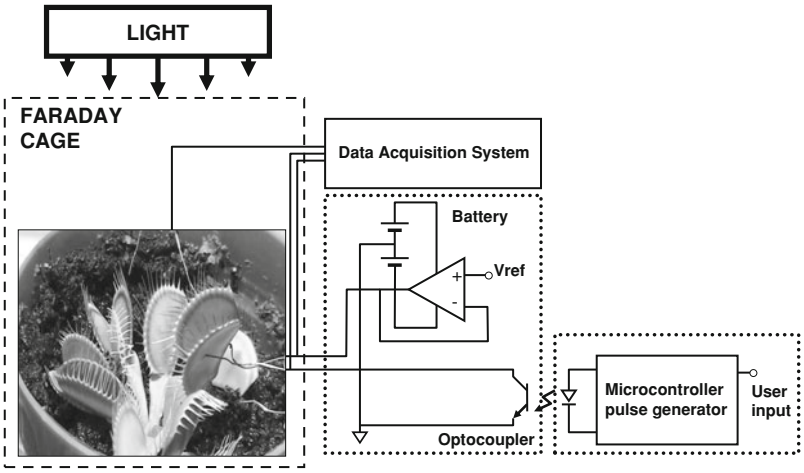

Fig. 2.6 Experimental setup for direct current electrostimulation of a plant with optical isolation

the pulse that results in much faster recharging of the capacitor. A separate battery was used to eliminate high-frequency interference of the pulse generator system.

Using our new DC electrostimulation system, it was evident that the application of an electrical stimulus between the midrib (positive potential) and a lobe (negative potential) causes the Venus flytrap to close the trap without any mechanical stimulation in 0.3 s after electrical stimulation (Volkov et al. 2007). The average stimulation pulse voltage sufficient for rapid closure of the Venus flytrap was 1.50 V (standard deviation is 0.01 V, $n = 50$) for 1 s. The inverted polarity pulse with negative voltage applied to the midrib could not close the plant. We were unable to open the plant by applying impulses in the same voltage range with different polarities for pulses of up to 100 s.

The primary objective of our experiments was to precisely determine the conditions of the charged electrical stimulation that generate a given biological effect. We implemented two types of electrostimulation: a manual switch and a custom made specific controller. Manual stimulation is convenient for single stimulation because it does not require additional equipment. It was implemented using a double pole double throw (DPDT) switch to connect the known capacitor to the voltage source during charging and then to the plant during plant stimulation to induce a response. However, manual switching does not allow precise control of timing of the stimulation. Therefore, we designed and implemented a custom plant stimulator to allow multiple stimulations with precise control of timing and voltage during stimulation. The plant stimulator is a battery-powered portable device controlled by a low-power microcontroller, MSP430F1611 (Texas Instruments, Texas, USA). A specialized PC program allows flexible configuration of the controller and communicates with the controller through optically isolated USB interface. During each stimulation cycle, the controller charges capacitor with

predefined voltage using integrated digital to analog (DA) converter of the microcontroller. A dual integrated analog switch controlled by the microcontroller connects the capacitor to DA converter during charging and to the plant during stimulation, allowing stimulation with microsecond resolution.

Each pulse can be controlled with resolution of 30 μs. The stimulation voltage can be set in steps of 0.6 mV to maximum voltage of 2.5 V. After charging, the capacitor with capacitance C charged with voltage V_s contains the amount of charge equal to $Q_1 = C\ V_s$ if the voltage after stimulation falls to V_{ps} the remaining charge will be $Q_2 = C\,V_{ps}$. Therefore, the stimulation delivered charge $\Delta Q = Q_1 - Q_2 = C(V_s - V_{ps})$. A dual integrated SPDT analog switch is controlled by the microcontroller and connects the capacitor to DA converter during charging and to the plant during stimulation. After N stimulations, the total amount of charge delivered is equal to $Q_s = C \cdot \sum_{i=1}^{N} (V_i - V_{pi})$. The proposed approach can therefore precisely define stimulation timing and charge. For a given capacitance of the stimulation capacitor, the user can select the number of stimulations N and the stimulation period.

For each stimulation, the capacitor was connected to electrodes in the plant until complete discharge and then disconnected from the electrodes. The following experiments with different conditions were performed at least 5 min later, although there was no noticeable difference in response for different time periods between stimulations. Voltage in the plant was measured between experiments, but no additional effects were detected between experiments. Electrodes remained in the plant between experiments.

It is possible to estimate charge $Q = UC$, electrical current $I = -\mathrm{d}Q/\mathrm{d}t$, work $W = U^2C/2$, power $P = UI$, and resistance $R = U/I$ from the time dependence of a capacitor discharge in a plant tissue as it is shown in Fig. 2.7 for a capacitor discharge in the Venus flytrap.

The charge stimulation method (Volkov et al. 2008a, b, 2009a, b, 2010a, b, c, d) was used to estimate, with high precision, the amount of electrical energy necessary to induce a response.

2.3.2.1 Mathematical Treatment of a Capacitor Discharge in Passive Electrical Circuits in Plants Developed by Professor V. S. Markin

If a capacitor of capacitance C with initial voltage U_0 is discharged during time t through a resistor R (Fig. 2.8a), the voltage across the capacitor decreases exponentially with time t:

$$U(t) = U_0 \cdot e^{-t/\tau} \tag{2.7}$$

where $\tau = \mathrm{RC}$ denotes the time constant and U_0 is the initial voltage of a capacitor (Feynman et al. 1963). Equation 2.7 in logarithmic form reads:

$$\log_{10} U(t) = \log_{10} U_0 - t/2.3 \tag{2.8}$$

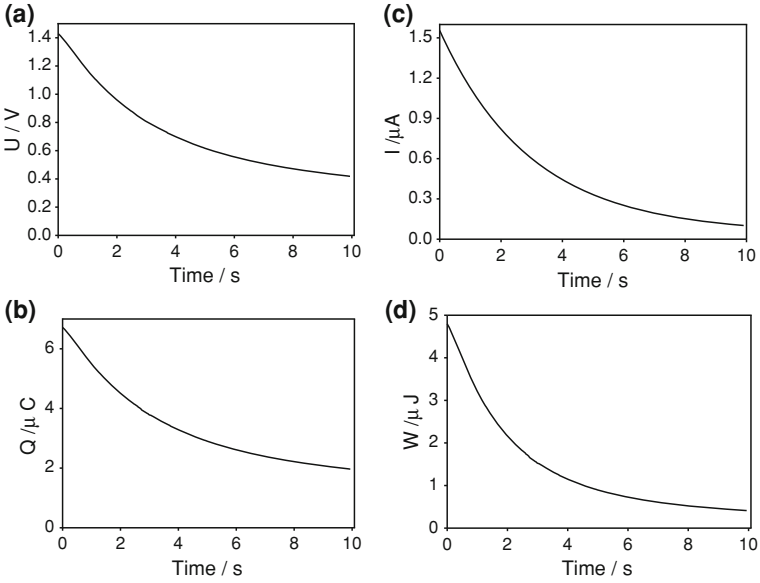

Fig. 2.7 Time dependencies of voltage U **a** charge Q **b** electrical current I **c**, and electrical energy W **d** during electrostimulation of the Venus flytrap upper leaf by 4.7 μF charged capacitor with initial voltage U_0 of 1.5

The time constant τ can be determined from the slope of this linear function. At $\tau = RC$, the capacitor charge is reduced to CU_0e^{-1}, which is about 37% of its initial charge. The voltage across the capacitor decreases exponentially from the initial value U_0 to zero. As the capacitance or resistance increases, the time of the capacitor discharge increases according to Eq. 2.7.

Professor V. S. Markin developed a mathematical treatment of a capacitor discharge in passive electrical circuits in plants (Volkov et al. 2010c). It was observed that capacitor discharge through the *Mimosa pudica* petiole has a two-exponential character (Volkov et al. 2010c). Therefore, the electrical circuit can be modeled as it is shown in Fig. 2.8b. In our experiment the capacitor C_1 was charged to voltage U_0 and the circuit was closed.

After closing the circuit, the electrical potentials U_1 and U_2 at capacitors C_1 and C_2 depend on time according to the equations:

$$\begin{cases} C_1 \frac{dU_1}{dt} = -\frac{1}{R_1}(U_1 - U_2) \\ C_2 \frac{dU_2}{dt} = -\frac{1}{R_1}U_1 - \left(\frac{1}{R_1} + \frac{1}{R_2}\right)U_2 \end{cases} \tag{2.9}$$

with initial conditions

$$U_1[0] = U_0, \quad U_2[0] = 0 \tag{2.10}$$

It is convenient to introduce parameters of time:

$$\theta_1 = R_1 C_1, \quad \theta_2 = R_2 C_2, \quad \theta_3 = R_2 C_1 \tag{2.11}$$

Voltage U_2 can be excluded from the system of Eq. 2.9 giving the single equation for U_1:

$$\theta_1 \theta_2 \frac{\mathrm{d}^2 U_1}{\mathrm{d}t^2} + (\theta_1 + \theta_2 + \theta_3) \frac{\mathrm{d}U_1}{\mathrm{d}t} + U_1 = 0 \tag{2.12}$$

Solving this equation one can find the time course of U_1:

$$\begin{aligned} U_1(t) = U_0 \Bigg\{ & \left[\frac{-\theta_1 + \theta_2 - \theta_3}{\sqrt{-4\theta_1\theta_2 + (\theta_1 + \theta_2 + \theta_3)^2}} + 1 \right] \\ & \times \mathrm{Exp}\left[-\frac{t\left(\theta_1 + \theta_2 + \theta_3 + \sqrt{-4\theta_1\theta_2 + (\theta_1 + \theta_2 + \theta_3)^2} \right)}{2\theta_1\theta_2} \right] \\ & + \left[\frac{\theta_1 - \theta_2 + \theta_3}{\sqrt{-4\theta_1\theta_2 + (\theta_1 + \theta_2 + \theta_3)^2}} + 1 \right] \\ & \times \mathrm{Exp}\left[-\frac{t\left(\theta_1 + \theta_2 + \theta_3 - \sqrt{-4\theta_1\theta_2 + (\theta_1 + \theta_2 + \theta_3)^2} \right)}{2\theta_1\theta_2} \right] \Bigg\} \end{aligned} \tag{2.13}$$

If the experimental dependence can be approximated with function

$$U(t) = A_1 \, \mathrm{e}^{-\frac{t}{\tau_1}} + A_2 \, \mathrm{e}^{-\frac{t}{\tau_2}} \tag{2.14}$$

and parameters A_1, A_2, τ_1, and τ_2 can be determined from the experiment, then one can evaluate the elements of the equivalent circuit in Fig. 2.8b.

To find parameters θ_1, θ_2, θ_3 simultaneously, Markin solved the set of nonlinear equations derived from comparison of Eqs. 2.13 and 2.14:

$$\begin{aligned} A_1 &= U_0 \left[\frac{-\theta_1 + \theta_2 - \theta_3}{\sqrt{-4\theta_1\theta_2 + (\theta_1 + \theta_2 + \theta_3)^2}} + 1 \right] \\ \frac{1}{\tau_1} &= \frac{\theta_1 + \theta_2 + \theta_3 + \sqrt{-4\theta_1\theta_2 + (\theta_1 + \theta_2 + \theta_3)^2}}{2\theta_1\theta_2} \\ \frac{1}{\tau_2} &= \frac{\theta_1 + \theta_2 + \theta_3 - \sqrt{-4\theta_1\theta_2 + (\theta_1 + \theta_2 + \theta_3)^2}}{2\theta_1\theta_2} \end{aligned} \tag{2.15}$$

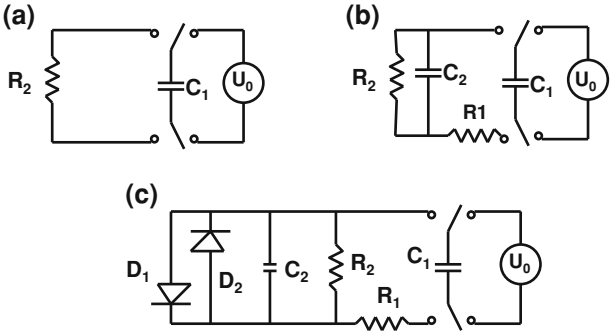

Fig. 2.8 Electrical equivalent schemes of a capacitor discharge in a plant tissue. Abbreviations: C_1 charged capacitor from voltage source U_0; C_2 capacitance of plant tissue; R resistance in plant tissue; D diode as a model of a voltage-gated channel

Finding from here θ_1, θ_2, and θ_3 and using the set of Eq. 2.11, one can determine the value of elements C_2, R_1, R_2 in the equivalent circuit shown in Fig. 2.8b. Volkov et al. (2010c) estimated these parameters in the *M. pudica* petiole.

Another interesting parameter is input resistance that can be defined as

$$R_{\text{input}} = -\frac{U_1}{C_1 \frac{\mathrm{d}U_1}{\mathrm{d}t}} \tag{2.16}$$

This parameter is also often analyzed in electrical impedance spectroscopy studies of biological tissues (Laarabi et al. 2005; Zhang and Willison 1991; Wang et al. 1994). However, there is a problem with interpretation of electrical impedance method, because a few different equivalent circuit models can have identical impedances (McAdams and Jossinet 1996).

2.3.3 Patch Clamp and Electrochemical Impedance Methods

The most frequently used methods for the evaluation of electrical circuits in plants are patch clamps, electrochemical impedance measurement, and electric charge stimulation. The patch clamp method can be used to study electrical characteristics of individual ionic channels in a biological membrane in vitro. Pipette-based recording of membrane currents is the mainstay in the characterization of cellular ion channels. Traditional patch clamp recording is accomplished by using a micromanipulator to position the tip of a glass pipette against the membrane of a cell. In voltage clamp mode, the membrane is clamped to a preset potential, and the current required maintaining this potential is recorded. Current recordings with different electrical protocols and in the presence of different reagents are used to characterize ion channel properties.

The electrochemical impedance method measures static electrical parameters, such as resistance and capacitance, at high-frequency alternative currents (AC). However, different electrochemical circuits can have the same electrochemical impedance.

The description of equivalent electrical circuits based on electrochemical impedance AC measurements is based on the researcher's intuition and can lead to various mistakes (McAdams and Jossinet 1996). Moreover, this method cannot characterize dynamic changes and nonlinear events, such as ion channel opening and closing.

2.4 Plant Electrostimulation

2.4.1 Plant Movements Induced by DC Electrostimulation

Mechanical movements in *M. pudica* were induced by very high applied voltages (Balmer and Franks 1975; Bose 1918; Gardiner 1888; Jonas 1970; Ritter 1811). Balmer and Franks (1975) briefly applied 200–400 V between the soil and the primary pulvinus to measure the contractile characteristics of a petiole. They estimated that the threshold voltage was about 25 V with any electrode polarity. Jonas (1970) used a 0.5 μF capacitor charged by 50, 100, and 150 V for electrostimulation and found that there were oscillations of leaves and fast petiolar movement after the application of an electrical shock. When Yao et al. (2008) applied 9 V to *M. pudica*, the petioles bent downward and the pinnae closed. Volkov et al. (Volkov et al. 2010e) investigated the mechanical movements of the pinnae and petioles in *M. pudica* induced by the electrical stimulation of a pulvinus, petiole, secondary pulvinus, or pinna by low electrical voltage and charge (Fig. 2.9). The threshold value was 1.3–1.5 V of applied voltage and 2–10 μC charge for the closing of the pinnules. Both voltage and electrical charge are responsible for the electrostimulated closing of a leaf (Volkov et al. 2010a, b, c, d).

The electrical stimulus between a midrib and a lobe closes the Venus flytrap leaf by activating motor cells without mechanical stimulation of trigger hairs (Markin et al. 2008; Volkov et al. 2007, 2008a, b, 2009a, b). The closing time of the Venus flytrap by electrical stimulation is 0.3 s, the same as mechanically induced closing. The Venus flytrap can accumulate small subthreshold charges, and when this threshold value is reached, the trap closes. Ion channel blockers such as Ba^{2+} and TEACl as well as uncouplers such as FCCP, 2,4-dinitrophenol and pentachlorophenol dramatically decrease the speed of the trap closing (Volkov et al. 2008c). Electrical stimulation can be used to study mechanisms of fast activity in motor cells of the plant kingdom.

2.4.2 DC Electrostimulation of Plants Can Induce Gene Expression, Enzymatic Systems Activation, Electrical Signaling, and Influences on Plant Growing

Excitability is a fundamental property that plants exhibit at the whole plant, tissue, and cellular levels. This property allows the cells, tissues, and organs of plants to

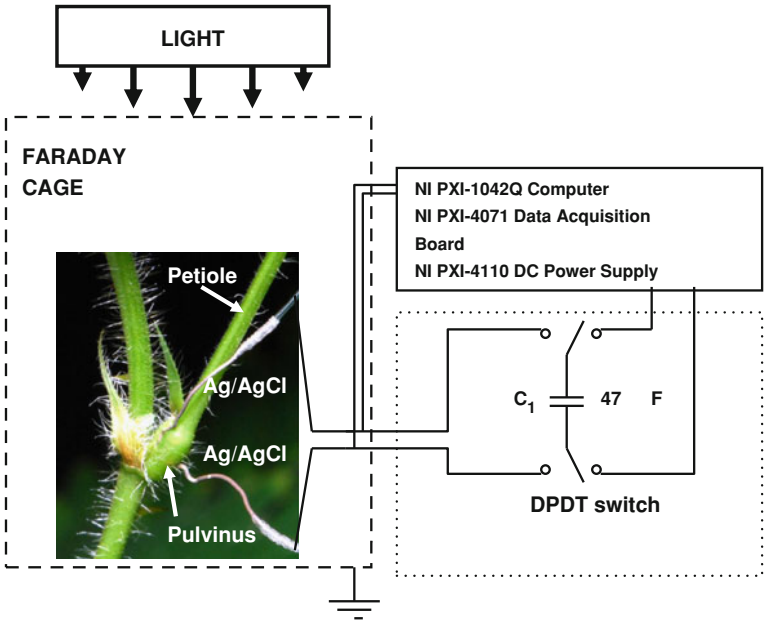

Fig. 2.9 Experimental setup for plant electrostimulation using the charge stimulation method and electrical signal measurements. We used PXI (PCI eXtensions for Instrumentation), a rugged PC-based platform, as a high-performance measurement and automation system (*National Instruments*, *Texas*)

operate in concert to adapt its internal conditions and external reactions in response to environmental stimulants referred to as irritants. The excitation waves, or action potentials, in higher plants are thought to be the mechanism behind intercellular and intracellular communication. Action potentials are signals caused by the depolarization of cellular membranes. Mechanical, physical, or chemical irritants affect not only the location of occurrence, but these irritants may also affect the entire plant as well. In plant species, the velocity of electrical signals depends on many factors, including the intensity of the irritation, temperature, chemical treatment, or mechanical wounding. The excitation reaction may travel between the top of the stem and the root in either direction.

Plant electrostimulation can have influence on the growth of plants (Takamura 2006). Mizuguchi et al. (1994) applied 1 V to the cultured solution and it accelerated by 30% the growth of bean sprouts. Goldsworthy (2006) described in his review how natural and artificial electrical fields stimulate plant growth in the electroculture experiments. Electrical fields can activate growth-promoting genes (Goldsworthy 2006). Electroculture experiments show that electrical fields from the aurora borealis are responsible for green and healthy vegetation in Arctic (Lemström 1904). Goldsworthy (2006) suggested that "plants seem to be using the very strong electrostatic fields associated with thunderstorms as signal to let them make the best use of the rain."

Fromm and Spanswick (1993) measured action potentials induced by electrostimulation of willow shoots. The threshold value of electrical stimulation was function of duration of electrical stimuli (6 V during 1 s, 3–4 V during 2 s or 10 nA in 1 s, 3 nA in 2 s, 2 nA during 4 s). Such dependence on time shows that both voltage and electrical charge are important for the plant electrical response. We can estimate the threshold charge of 6–10 nC by multiplying the threshold current by time of polarization. Amplitude of action potentials was 30–50 mV with velocity of 2 cm/s.

Inaba et al. (1995) applied DC current of 1–3 mA to cucumber (*Cucumis sativus* L.) and found induction of ethylene synthesis and activation of 1-aminocyclopropane-1-carboxylic acid synthase. Inaba et al. (1995) also evaluated parameters of the equivalent electrical circuit of plant tissues.

Herde et al. (1995, 1996) found that electrical current application (10 V, 30 s) activated *pin*2 gene expression in tomato plants and increases endogenous level of abscisic acid.

Stanković and Davies (1996, 1997) demonstrated that electrical stimulation of tomato plants by 9 V during 3–4 s occasionally induces "genuine" action potentials with amplitude of 40 mV and speed of 3.5–4.5 mm/s and elicits systemic *pin*2 gene expression. Propagation of electrical signals in response to electrostimulation was found in 20% of tomato plants only (Stankovic and Davies 1996, 1997). Authors did not analyze the threshold level of a stimulation voltage and possible dependence of action potential on amplitude and polarity of applied voltage. Stankovic and Davies (1996, 1997) found after 9 V electrostimulation that "5-fold or greater increase in *pin*2 mRNA levels occurs within 1 h".

Mishra et al. (2001) studied action potential propagations with velocity of 270 m/s and a latency of 400 μs from root to shoot in *Sorghum bicolor* evoked by electrostimulation. The threshold current was 100 μA during 0.3 ms. These values correspond to the threshold charge of 30 nC. In 7-day-old seedling the threshold charge was 0.45 μC. According to the strength-duration curve of *S. bicolor* seedling the threshold charge varies from 30 to 3 μC (Mishra et al. 2001).

Dziubinska et al. (2001) applied electrical stimuli of 1–2 V during 5 s to the basal part of the stem of *Helianthus annuus* and recorded propagation of action potentials along the stem with an amplitude of 42 mV with speed of 0.18 cm/s. Authors were unable to evoke action potentials by electrical stimulation of leaves (Dziubinska et al. 2001).

Krol et al. (2006) triggered action potentials in the Venus flytrap by electrical stimuli up to 4 V.

Favre and Agosti (2007) described voltage-dependent "action potentials" in *Arabidopsis thaliana* induced by 3–18 V pulses. Amplitude of these "action potentials" was between 10 and 80 mV with an absolute refractory period of 20 min and a speed of propagation of 0.8–1.4 mm/s. Amplitude and velocity of electrical responses was a function of applied voltage.

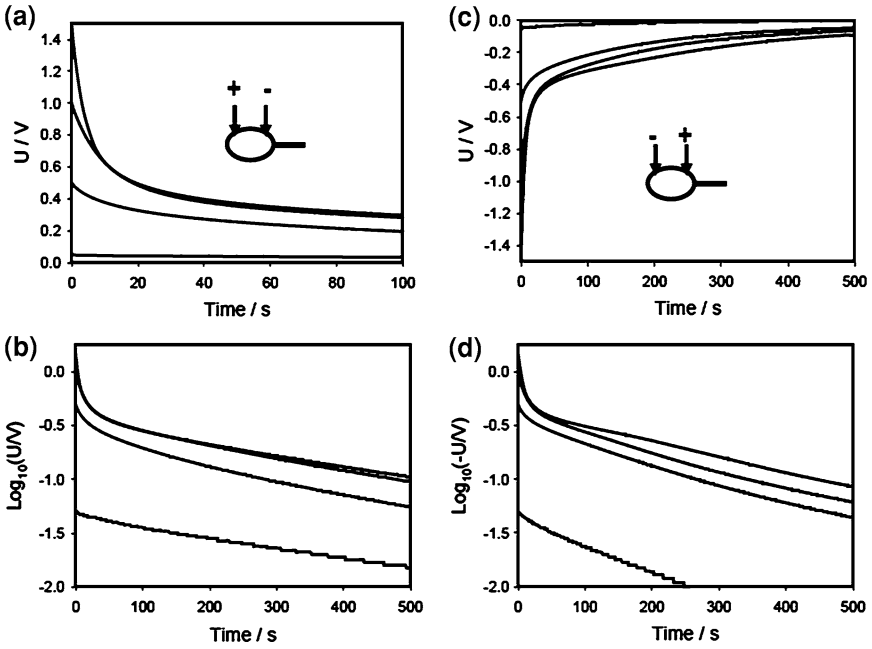

Fig. 2.10 Time dependence of electrical discharge in *M. pudica* pulvinus between electrodes located along the pulvinus and connected to 47 μF charged capacitor (**a**, **c**) Time dependence of electrical discharge in the *M. pudica's* pulvinus between electrodes located along the pulvinus and connected to a charged capacitor in logarithmic coordinates (**b**, **d**)

2.4.3 Anisotropy and Nonlinear Properties of Biologically Closed Electrochemical Circuits in Plants

Electrical circuits in Fig. 2.8a, b are not sensitive to the polarity of applied voltage. We found that after threshold value of electrostimulating potential there is a strong deviation in logarithmic coordinates from Eq. 2.8 predictions and plant electrical responses depend on polarity of applied voltage (Fig. 2.10). The deviation of a capacitor discharge from a linear dependence in logarithmic coordinates can be described by the equivalent electrical schemes shown in Fig. 2.8b, c (Volkov et al. 2009b, 2010a b, c, d). If the capacitor discharge is represented by two-exponential functions and does not depend on polarity of electrodes in the plant tissue, the deviation from linear dependence can be described by Fig. 2.8b. If the response changes with the polarity of stimulation, a rectifier-based model represented in Fig. 2.8c must be used. Kinetics of a capacitor discharge depends on the polarity of electrodes in the *Aloe vera* leaf, Venus flytrap, and *M. pudica* (Figs. 2.10 and 2.11). Figure 2.11 shows the difference in the kinetics of a capacitor discharge as a function of the polarity of stimulation as represented in Fig. 2.10a, c. Dependence of a capacitor discharge on the polarity of electrodes in the *M. pudica* leaf, shown

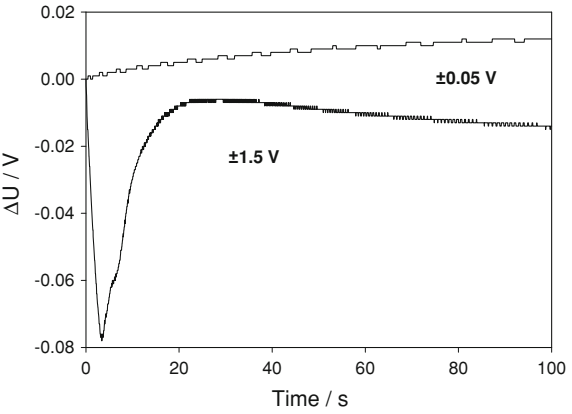

Fig. 2.11 Time dependence of voltage differences (Fig. 2.10a + c) during electrical discharge in the *M. pudica's* pulvinus between electrodes of different polarities located along the *M. pudica* pulvinus and connected to 47 μF charged capacitor

in Figs. 2.10 and 2.11, can be explained by a change in resistivity with applied potential due to opening of ion channels, which can be modeled by diodes in Fig. 2.8c. Opening of voltage-gated channels induce the effect of electrical rectification shown in Fig. 2.11. We found similar rectification effects in the Venus flytrap (Volkov et al. 2009b), *A. vera* (Volkov et al. 2011a, b), and *M. pudica* (Volkov et al. 2010a, b, c, d, e, 2011a). We modeled voltage-gated channels using silicon rectifier diode and reproduced experimental dependencies of a capacitor discharge in plant tissue (Volkov et al. 2009b).

2.4.4 Circadian Variations in Biologically Closed Electrochemical Circuit in Plants

The circadian clock regulates a wide range of electrophysiological and developmental processes in plants. The circadian clock is an endogenous oscillator with a period of approximately 24 h; its rhythm is linked to the light–dark cycle. Molecular mechanism underlying circadian clock function is poorly understood, although it is widely accepted for both plants and animals that are based on circadian oscillators. The circadian clock in plants is sensitive to light, which resets the phase of the rhythm. The circadian clock was discovered by De Mairan (1729) in his first attempt to resolve experimentally the origin of rhythm in the leaf movements of *M. pudica*. This rhythm continued even when *M. pudica* was maintained under continuous darkness. *M. pudica* is a nyctinastic plant that closes its leaves in the evening; the pinnules fold together and the whole leaf droops downward temporarily until sunrise. The leaves open in the morning due to a circadian rhythm, which is regulated by a biological clock with a cycle of about 24 h. During photonastic movement in *M. pudica*, leaves recover their daytime position. During a scotonastic period, the primary pulvini straighten up and pairs of pinnules fold together about the tertiary pulvini. The closing of pinnae depends upon the presence of phytochrome in the far-red absorbing form.

Volkov et al. (2011a,c) found, for the first time, the direct influence of a circadian clock on biologically closed electrochemical circuits in vivo using the Charge Stimulating Method. The electrostimulation of a sensitive plant *M. pudica* and *A. vera* was provided with different timing and different voltages. *A. vera* (L.) is a member of the Asphodelaceae (Liliaceae) family with crassulacean acid metabolism (CAM). In *A. vera*, stomata are open at night and closed during the day. CO_2 acquired by *A. vera* at night is temporarily stored as malic and other organic acids, and is decarboxylated the following day to provide CO_2 for fixation in the Benson-Calvin cycle behind closed stomata.

A. vera is a model for the study of plant electrophysiology with crassulacean acid metabolism.

Resistance between Ag/AgCl electrodes in the leaf of *A. vera* was higher during the day than at night. Discharge of the capacitor in *A. vera* at night was faster than during the day. Discharge of the capacitor in a pulvinus of *M. pudica* was faster during the day. The biologically closed electrical circuits with voltage-gated ion channels in *M. pudica* are also activated the next day, even in the darkness. These results show that the circadian clock can be maintained endogenously and has electrochemical oscillators, which can activate ion channels in biologically closed electrochemical circuits. Initial difference in the speed of the capacitor discharge (faster during the day), can be explained by activation of ion channels, equivalent to the high rectification effect. This effect depends on the applied stimulation voltage.

Isolated pulvinar protoplasts are responsive to light signals in vitro (Coté 1995; Kim et al. 1992, 1993). In the dark period, the closed inward-directed K^+ channels of extensor cells are opened within 3 min by blue light. Conversely, the inward-directed K^+ channels of flexor cells, which are open in the darkness, are closed by blue light. In the light period, however, the situation is more complex. Premature darkness alone is sufficient to close the open channels of extensor protoplasts, but both darkness and a preceding pulse of red light are required to open the closed channels in the flexor protoplasts (Kim et al. 1992, 1993).

The biologically closed electrical circuits with voltage-gated ion channels in *M. pudica* are activated the next day even in the darkness. This phenomenon can be caused by biological clock in *M. pudica*. The nonlinear effect of activation of electrical circuits during the daytime is stronger than during the next day in the darkness.

In contrast to *A. vera* the discharge of the capacitor in a pulvinus of *M. pudica* was faster during the day, because *A. vera* is a CAM plant.

Our results (Volkov et al. 2011a, c) demonstrate that the circadian clock can be maintained endogenously, probably involving electrochemical oscillators, which can activate or deactivate ion channels in biologically closed electrochemical circuits. This circadian rhythm can be related to the differences found in the membrane potentials during the day- and nighttime, which were found in different plants (Kim et al. 1992; 1993; Racusen and Satter 1975; Scott and Gulline 1975; Thomas and Vince-Prue 1997). The expression of many ion transporters in plants is regulated by the circadian rhythm (Lebaudy et al. 2008).

2.5 Conclusion

The information gained from plant electrostimulation can be used to elucidate the intracellular and intercellular communication in the form of electrical signals within plants. Monitoring the electrical signaling in higher plants represents a promising method to investigate electrical communication during environmental changes.

Acknowledgments This work was supported by the grant W911NF-11-1-0132 from the U.S. Army Research Office.

References

Balmer RT, Franks JG (1975) Contractile characteristics of *Mimosa pudica* L. Plant Physiol 56:464–467

Bertholon M (1783) De l'electricite des vegetaux: ouvrage dans lequel on traite de l'electricite de l'atmosphere sur les plantes, de ses effets sur leconomie des vegetaux, de leurs vertus medico. P.F. Didot Jeune, Paris

Bose JC (1907) Comparative electro-physiology, a physico-physiological study. Longmans, Green & Co, London

Bose JC (1913) Researches on irritability of plants. Longmans, London

Bose JC (1918) Life Movements in Plants. B.R. Publishing Corp, Delhi

Bose JC (1926) The Nervous mechanism of plants. Longmans, Green and Co., London

Bose JC (1928) The motor mechanism of plants. Longmans Green, London

Burdon-Sanderson J (1873) Note on the electrical phenomena which accompany stimulation of the leaf of *Dionaea muscipula*. Philos Proc R Soc Lond 21:495–496

Coté GG (1995) Signal transduction in leaf movement. Plant Physiol 109:729–734

Davies E (2006) Electrical signals in plants: facts and hypothesis. In: Volkov AG (ed) Plant electrophysiology—Theory & methods. Springer, Berlin, pp 407–422

De Mairan M (1729) Observation botanique. Histoire de l'Academie Royale de Sciences, Paris, pp 353–356

Dziubinska H, Trebacz K, Zawadzki T (2001) Transmission route for action potentials and variation potentials in *Helianthus annuus* L. J Plant Physiol 158:1167–1172

Favre P, Agosti RD (2007) Voltage-dependent action potentials in Arabidopsis thaliana. Physiol Plant 131:263–272

Feynman RP, Leighton RB, Sands M (1963) The Feynman lectures on physics. Addison Wesley, Reading

Fromm J, Spanswick R (1993) Characteristics of action potentials in willow (*Salix viminalis* L.). J Exp Bot 44:1119–1125

Gardiner W (1888) On the power of contractility exhibited by the protoplasm of certain plant cell. Annals Botany 1:362–367

Goldsworthy A (2006) Effects of electrical and electromagnetic fields on plants and related topics. In: Volkov AG (ed) Plant electrophysiology—Theory and methods. Springer, Berlin, pp 247–267

Herde O, Atzorn R, Fisahn J, Wasternack C, Willmitzer L, Peña-Cortés H (1996) Localized wounding by heat initiates the accumulation of proteinase inhibitor II in abscisic acid-deficient plants by triggering jasmonic acid biosynthesis. Plant Physiol 112:853–860

Herde O, Peña-Cortés H, Fisahn J (1995) Proteinase inhibitor II gene expression induced by electrical stimulation and control of photosynthetic activity in tomato plants. Plant Cell Physiol 36:737–742

Houwink AL (1935) The conduction of excitation in *Mimosa pudica*. Recuril des Travaux Botaniques Neerlandais 32:51–91

Houwink AL (1938) The conduction of excitation in Clematis zeylanica and in *Mimosa pudica*. Annales du Jardin Botanique de Buitenzorg 48:10–16

Inaba A, Manabe T, Tsuji H, Iwamoto T (1995) Electrical impedance analysis of tissue properties associated with ethylene induction by electric currents in cucumber (*Cucumis sativus* L.) fruit. Plant Physiol 107:199–205

Jonas H (1970) Oscillations and movements of *Mimosa* leave due to electric shock. J Interdisciplinary Cycle Res 1:335–348

Keller R (1930) Der elektrische Factor des Wassertransporte in Luhte der Vitalfarbung. Ergeb Physiologie 30:294–407

Kim HY, Coté GG, Crain RC (1992) Effect of light on the membrane potential of protoplasts from Samanea saman pulvini. Involvement of K^+ channels and the H^+-ATPase. Plant Physiol 99:1532–1539

Kim HY, Coté GG, Crain RC (1993) Potasium channels in Samanea saman protoplasts controlled by phytochrome and the biological clock. Science 260:960–962

Krol E, Dziubinska H, Stolarz M, Trebacz K (2006) Effects of ion channel inhibitors on cold- and electrically-induced action potentials in *Dionaea muscipula*. Biol Plantarum 50:411–416

Ksenzhek OS, Volkov AG (1998) Plant energetics. Academic, San Diego

Laarabi S, Kinani KE, Ettouhami A, Limouri M (2005) In vivo impedance of the aerial organs of some mono- and dicotyledonous plants. CR Biol 328:253–262

Lebaudy A, Vavasseur A, Hisy E, Dreyer I, Leonhards N, Thibaud JB, Very AA, Simonneau T, Sentenac H (2008) Plant adaptation to fluctuating environment and biomass production are strongly dependent on guard cell potassium channels. Proc Natl Acad Sci 105:5271–5276

Lemström K (1904) Electricity in agriculture and horticulture. Electrician Publications, London

Markin VS, Volkov AG, Jovanov E (2008) Active movements in plants: mechanism of trap closure by *Dionaea muscipula* Ellis. Plant Signal Behav 3:778–783

McAdams ET, Jossinet J (1996) Problems in equivalent circuit modeling of the electrical properties of biological tissues. Bioelectrochem Bioenerg 40:147–152

Mishra NS, Mallick BN, Sopory SK (2001) Electrical signal from root to shoot in Sorghum bicolor: induction of leaf opening and evidence for fast extracellular propagation. Plant Sci 160:237–245

Mizuguchi Y, Watanabe Y, Matsuzaki H, Ikezawa Y, Takamura T (1994) Grouth acceleration of bean sprouts by the application of electrochemical voltage in a culturing bath. Denki Kagaku 62:1083–1085

Nordestrom BEW (1983) Biologically closed electrical circuits. Clinical, experimental and theoretical evidence for an additional circulatory system. Nordic Medical Publications, Uppsala

Ritter JW (1811) Electrische Versuche an der Mimosa pudica L. In Parallel mit gleichen Versuchen an Fröschen. Denkschr Köningl Akad Wiss (München) 2:345–400

Racusen R, Satter RL (1975) Rhytmic and phytochrome-regulated changes in transmembrane potential in Samanea pulvini. Nature 255:408–410

Scott BIH, Gulline HF (1975) Membrane changes in a circadian system. Nature 254:69–70

Shannon CE (1949) Communication in the presence of noise. Proc Inst Radio Eng 37:10–21

Sinukhin AM, Britikov EA (1967) Action potentials in the reproductive system of plant. Nature 215:1278–1280

Stankovic B, Davies E (1996) Both action potentials and variation potentials induce proteinase inhibitor gene expression in tomato. FEBS Lett 390:275–279

Stankovic B, Davies E (1997) Intercellular communication in plants: electrical stimulation of proteinase inhibitor gene expression in tomato. Planta 202:275–279

Takamura T (2006) Electrochemical potential around the plant root in relation to metabolism and growth acceleration. In: Volkov AG (ed) Plant electrophysiology—Theory & methods. Springer, Berlin, pp 341–374

Thomas B, Vince-Prue D (1997) Photoperiodism in plants. Academic, San Diego

Volkov AG (2000) Green plants: electrochemical interfaces. J Electroanal Chem 483:150–156

Volkov AG (2006a) Electrophysiology and phototropism In: Balushka F, Manusco S, Volkman D (eds) Communication in plants. Neuronal aspects of plant life. Springer, Berlin, pp 351–367

Volkov AG (ed) (2006b) Plant electrophysiology—Theory and methods. Springer, Berlin

Volkov AG, Adesina T, Jovanov E (2008a) Charge induced closing of Dionaea muscipula Ellis trap. Bioelectrochem 74:16–21

Volkov AG, Adesina T, Markin VS, Jovanov E (2007) Closing of Venus flytrap by electrical stimulation of motor cells. Plant Signal Behav 2:139–144

Volkov AG, Adesina T, Markin VS, Jovanov E (2008b) Kinetics and mechanism of *Dionaea muscipula* trap closing. Plant Physiol 146:694–702

Volkov AG, Baker K, Foster JC, Clemmens J, Jovanov E, Markin VS (2011a) Circadian variations in biologically closed electrochemical circuits in *Aloe vera* and *Mimosa pudica*. Bioelectrochem 81:39–45

Volkov AG, Carrell H, Adesina T, Markin VS, Jovanov E (2008c) Plant electrical memory. Plant Signal Behav 3:490–492

Volkov AG, Carrell H, Baldwin A, Markin VS (2009a) Electrical memory in Venus flytrap. Bioelectrochem 75:142–147

Volkov AG, Carrell H, Markin VS (2009b) Biologically closed electrical circuits in Venus flytrap. Plant Physiol 149:1661–1667

Volkov AG, Deamer DW, Tanelian DL, Markin VS (1998) Liquid interfaces in chemistry and biology. Wiley, New York

Volkov AG, Foster JC, Ashby TA, Walker RK, Johnson JA, Markin VS (2010a) *Mimosa pudica*: electrical and mechanical stimulation of plant movements. Plant Cell Environ 33:163–173

Volkov AG, Foster JC, Baker KD, Markin VS (2010b) Mechanical and electrical anisotropy in *Mimosa pudica*. Plant Signal Behav 5:1211–1221

Volkov AG, Foster JC, Jovanov E, Markin VS (2010c) Anisotropy and nonlinear properties of electrochemical circuits in leaves of *Aloe vera* L. Bioelectrochem 81:4–9

Volkov AG, Foster JC, Markin VS (2010d) Signal transduction in *Mimosa pudica*: Biologically closed electrical circuits. Plant, Cell Environ 33:816–827

Volkov AG, Foster JC, Markin VS (2010e) Molecular electronics in pinnae of *Mimosa pudica*. Plant Signal Behav 5:826–831

Volkov AG, Foster JC, Jovanov E, Markin VS (2011b) Anisotropy and nonlinear properties of electrochemical circuits in leaves of *Aloe vera* L. Bioelectrochem 81:4–9

Volkov AG, Pinnock MR, Lowe DC, Gay MS, Markin VS (2011c) Complete hunting cycle of *Dionaea muscipula*: consecutive steps and their electrical properties. J Plant Physiol 168:109–120

Volkov AG, Wooten JD, Waite AJ, Brown CR, Markin VS (2011d) Circadian rhythms in electrical circuits of *Clivia miniata*. J Plant Physiol 168:1753–1760

Volkov AG, O'Neal L, Ebere LC, McIntyre R, Volkova-Gugeshashvili MI, Markin VS (2012) Propagation and collision of nonlinear responses in *Aloe vera* L. and *Arabidopsis thaliana*. Plant Signal Behav 7:5 (in Press)

Wang J, Zimmermann U, Benz R (1994) Contribution of electrogenic ion transport to impedance of the algae *Valonia utricularis* and artificial membranes. Biophys J 67:1582–1593

Yao H, Xu Q, Yuan M (2008) Actin dynamics mediates the changes of calcium level during the pulvinus movement of *Mimosa pudica*. Plant Signal Behav 3:954–960

Zhang MIN, Willison JHM (1991) Electrical impedance analysis in plant tissues: a double shell model. J Exper Bot 42:1465–1475